Multiscale Network Model for Evaluating Global Outbreak Control Strategies

Nathan Chen, David Rey, and Lauren Gardner

High volumes of passenger air travel increase the risk of infectious disease epidemics and pandemics. Regional preparedness planning for large-scale outbreaks requires models that are able to capture outbreak dynamics within a control policy evaluation framework. Previous studies focused on either modeling outbreak dynamics or optimizing outbreak control decisions; this paper proposes an integrated approach that combines both aspects. A multiscale epidemic outbreak model is introduced that is designed to capture the infection dynamics at both the local (city) scale and the global (air travel) scale. A bilevel decision-making framework is then proposed to identify the optimal set of outbreak control policies, while accounting for local and global outbreak dynamics. The model is implemented for a case study in which a hypothetical epidemic outbreak is assumed to emerge from within the United States, and different control resource allocation strategies are explored and evaluated. The results highlight the importance of accounting for outbreak dynamics within the decision-making process and provide insight into the design and efficiency of a range of control strategies. This research is an initial effort to be followed by further research on the design of outbreak control strategies by using optimization algorithms under this framework.

The scale and connectivity of the global air travel network introduce a new dimension of risk for infectious disease spread. Today, infected individuals can easily travel to new regions where the local public health authorities may not be prepared, thus increasing the risk of pandemics. Historical examples include the 2003 SARS outbreak in Hong Kong, which spread to 37 countries over a period of 6 months, and the swine flu outbreak in 2009, which resulted in approximately 61 million people being infected worldwide within a single year.

Epidemic control measures can be applied to the air travel network to minimize the risk of large-scale contagion episodes. As an example, in the height of the Ebola outbreak in 2014, an extra layer of temperature screening was applied to passengers entering the United States from the three most impacted West African countries. Five airports were selected for the extra screening: JFK Airport in New York, Newark Liberty International Airport in New Jersey, Chicago O'Hare International Airport, Washington Dulles International Airport, and Hartsfield-Jackson Atlanta International Airport (*1*). From the perspective of policy decision makers, such as the Centers for Disease Control and Prevention, it is critical to assess the cost and effectiveness of such control measures at both the local (city) and global (national and international) levels. Therefore, it is prudent to investigate the complete dynamics of the infection, which includes both local and interregional transmission, to better understand the spreading behavior and design the most effective outbreak control measures.

It is the purpose of this research to develop a network modeling framework that can be used to evaluate the impact of outbreak control policies and rank them with respect to both performance and cost. To achieve this, a multiscale epidemic outbreak model was developed that captures the infection dynamics at both the local and global scales. The epidemic outbreak model was then used to evaluate a range of control policies that vary in their allocation of resources. This framework is proposed in the form of a bilevel optimization formulation that accounts for local and global outbreak dynamics within the decision-making process. On the basis of the results from the model, the most cost-efficient set of strategies can be identified.

The developed model is applied to a case study by using the worldwide air travel network, where the control policy considered is passenger screening at U.S. airports, and the control strategy performance is based on the resulting size of the outbreak at a given point in the future.

STATE OF THE ART

The literature review is conducted in two parts, each corresponding to a major contribution of this work. The first section includes a discussion of previous works that seek to capture the dynamics of epidemic outbreak at both local and global levels, which are used for predicting future epidemic spread. The second section addresses the set of previous works that incorporate an optimization process to inform epidemic control decisions.

Outbreak Dynamics Models

The fundamental epidemic model was developed by Kermack and McKendrick (*2*). This compartmental model is used to represent the evolution of an outbreak in a given population over time by using a set of differential equations and specifies the proportion of the population in each possible state that an individual can assume: susceptible (S), infected (I), and recovered (R). The SIR model assumes a homogeneous population mix. This model assumes that disease transmission is a mass action process. Hence an important underlying assumption of the model is that each individual has the same opportunity of coming into contact with any other individual.

The SIR model is often only used to model the transmission dynamics within a single homogeneous population. For a heterogeneous network consisting of multiple linked populations, for instance, cities connected by the air travel network, a more detailed model that accounts for the scale-free properties of the network

School of Civil and Environmental Engineering, University of New South Wales, Sydney, New South Wales 2052, Australia. Corresponding author: N. Chen, z3284800@zmail.unsw.edu.au.

Transportation Research Record: Journal of the Transportation Research Board, No. 2626, 2017, pp. 42–50.
http://dx.doi.org/10.3141/2626-06

structure is necessary (*3*). Simulation-based (*4–7*) and analytical epidemic models (*8–10*) have both been developed to analyze different epidemic spreading processes on the basis of the air traffic network. These models are useful for planning purposes and are developed to predict expected epidemic spreading behaviors for a range of outbreak scenarios.

Properties of the air traffic network structure were also studied in detail to generate analytical insights and predictions on the path of the epidemic spread. The work by Gardner et al. (*11*) and Brockmann and Helbing (*12*) are examples of this type of model. Gardner et al. used the current epidemic reports and the air traffic network structure to infer the most likely path that the epidemic has taken. Brockmann and Helbing explored paths in the network to compute the likelihood of nodes in the network being infected from a source node. Similar predictive models were also proposed by Gardner and Sarkar (*13*) and Gardner et al. (*14*) on the airport importation risk of dengue. These predictive approaches combine outbreak information and air travel network properties and are valuable for epidemic risk assessment in the context of the global air travel network and policy decision making.

Outbreak Control Models

Optimal allocation of epidemic control resources within multiple independent populations has been studied by Richter et al. (*15*) and Brandeau et al. (*16*). Their models aim to minimize the number of people infected in the populations over a finite time horizon, by reducing the rate of contact between susceptible and infected individuals by employing epidemic prevention programs. Zaric and Brandeau (*17*) built on these models to develop a more general modeling framework, accounting for interactions and interventions between multiple populations. However, these interactions were modeled by assumed movement rates, and an example with four populations was given. The objective examined was to minimize the impact of infection occurring over a long-term horizon—up to multiple years. The application of control to a single population over multiple time periods has also been studied by Greenhalgh (*18, 19*), Blount et al. (*20*), and Müller (*21*). Zaric and Brandeau then combined these two types of models to develop a resource allocation model in which both multiple time periods and multiple populations are considered (*22*). In this work, the authors use a susceptible–infected–susceptible model (instead of an SIR model). Ndeffo Mbah and Gilligan explored a similar allocation problem using the SIR model (*23*). The inclusion of the recovered compartment (which was also accounted for in work reported here) increases the complexity of the model and optimization problem. The present study significantly differs from these previous studies by exploring the resource allocation problem in a network-based environment, where the structure of the network plays a critical role in the interaction of the populations.

The optimal allocation of control resources in the context of a travel network was explored by Deng et al. by using a bipartite network, assessing the effects of both vaccination and location travel restrictions (*24*). Other optimization strategies were developed by Cohen et al. (*25*), Borgs et al. (*26*), Chung et al. (*27*), Roy et al. (*28*), Gourdin et al. (*29*), and Preciado et al. (*30*). These models do not assume subpopulations within nodes in the network. That is, the modeling frameworks used therein assume each node represents an individual, and network science metrics are often used to aid in optimization decision making. Chen et al. developed an optimization model by using air travel network data, but the population spreading dynamics within each node were not explored (*31*).

This study takes this research direction a step further by developing a multiscale network modeling framework for the purposes of evaluating different outbreak control strategies, while simultaneously capturing interactions between populations and also the local population infection dynamics. Thus this study combines the use of an outbreak dynamics model and an outbreak control model. Within the outbreak dynamics model, the structure of the passenger air travel network is used to connect different locations. In the outbreak control model, the effectiveness of different control policies is evaluated for both cost and performance (by using the outbreak dynamics model). The complete model is presented as a bilevel formulation in the next section.

PROBLEM FORMULATION

This section presents the mathematical formulation of the decision problem addressed in this paper. A bilevel optimization approach is proposed in which the lower (follower) level captures the reaction of the outbreak, whereas the upper (leader) level represents the resource allocation problem. This approach allows one to model the outbreak control problem as a decision problem while accounting for outbreak dynamics.

The proposed lower-level formulation is articulated with a multiscale structure: a local-scale SIR model is used to model outbreak dynamics at the city level and a global-scale network is used to model outbreak dynamics across the air traffic network. The upper-level decision problem addressed is that of finding the optimal allocation of outbreak control resources at the global level such that contagion risk is minimized subject to budget restrictions.

The outbreak model used to represent disease spread at the local scale is presented first and then there is a discussion on how this model is embedded within a larger global-scale structure representative of the air traffic network. Next a new formulation for the outbreak control problem is proposed.

Local-Scale Outbreak Model

The local-scale SIR model proposed to model the spread of infection within each individual region can be expressed in the following form, as proposed by Kermack and McKendrick (*2*):

$$\frac{dS}{dt} = -\frac{\beta IS}{N} \tag{1}$$

$$\frac{dI}{dt} = \frac{\beta IS}{N} - \gamma I \tag{2}$$

$$\frac{dR}{dt} = \gamma I \tag{3}$$

where S, I, and R are the number of individuals in each compartment at a particular time. The SIR model can be represented by ordinary differential equations summarized in Equations 1 through 3.

The model states the relationship between the current number of individuals in each compartment and the rate at which these compartments grow. The rate at which susceptible individuals are infected is related to the number of infected individuals in the population, the total population size, and the transmission rate β, which is the probability of an infection happening when an infected individual and a susceptible individual come into contact. The rate of the recovery of the infected individuals depends on γ, the recovery rate of the epidemic. The inverse of this value, $1/\gamma$, is the time it takes for an infected individual to recover from the infection.

Global-Scale Outbreak Model

The model used to represent outbreak behavior at the global scale (i.e., among different regions) is now presented. Let $G = (V, E)$ be a graph representing the air traffic network. The set of nodes V represents regions (e.g., cities) in which accessible airports exist, with a local population $N_{i,t}$ (within each region), where the subscript i is for node index and the subscript t is for time step (i.e., the population is allowed to fluctuate on the basis of seasonal travel patterns). The set of links E represents air travel routes between regions that carry air travel passenger flow f_{ij} between each node pair (i, j), where j belongs to $\theta(i)$, the set of nodes with direct links to node i, which is referred to as neighbors of i. With this notation, one can then denote f_i^+, the total number of incoming flows into a region node i:

$$f_i^+ = \sum_{j\in\theta(i)} f_{ij} \tag{4}$$

This notation will be useful when the epidemic control measures are discussed later. The propagation of infection between regions through these flows captures the interregional spreading dynamics.

Coupling Local and Global Outbreak Models to a Multiscale Model

Next the authors describe how the local-scale SIR model and the global-scale network model introduced are coupled into a multiscale epidemic spreading model, here referred to as multiscale outbreak model. The local-scale outbreak model describes the epidemic progression within each region (i.e., node of the air traffic network). Accordingly, one can index the number of susceptible, infected, and recovered individuals by node index i. It is also assumed that the contact rate β varies by region; hence β_i is denoted as the local contact rate. This assumption is important, because it is motivated by the observation that the rate of contact between people is a function of the population density in a region. In this work a linear relationship is assumed.

In addition, this paper proposes to model the infection on a discretized time scale, even though the original SIR model is a continuous time model. This approach is adopted to couple the local outbreak models with global outbreak dynamics. If the time step used in the discrete time model is small enough compared with the total modeling time scale, then the model will faithfully reflect the outbreak evolution. Let the set of discrete time steps be $T = \{0, 1, 2, \ldots, t_{\text{obs}}\}$, where t_{obs} is the observation time step at which one seeks to assess the outbreak state. Therefore, a time step subscript is added to the notations of the individuals in each compartment in each region too, and Equations 1, 2, and 3 become

$$S_{i,t+1} - S_{i,t} = -\frac{\beta_i I_{i,t} S_{i,t}}{N_{i,t}} \qquad \forall i \in V \qquad \forall t \in T \tag{5}$$

$$I_{i,t+1} - I_{i,t} = -\frac{\beta_i I_{i,t} S_{i,t}}{N_{i,t}} - \gamma I_{i,t} \qquad \forall i \in V \qquad \forall t \in T \tag{6}$$

$$R_{i,t+1} - R_{i,t} = \gamma I_{i,t} \qquad \forall i \in V \qquad \forall t \in T \tag{7}$$

where $S_{i,t}$, $I_{i,t}$, and $R_{i,t}$ are the number of individuals in each compartment S, I, and R at node i and time t, respectively.

Note that the rates of change of compartments are now expressed as finite differences from the previous time step. The changes in time step $t + 1$ are calculated on the basis of the condition of time step t. The recovery rate γ remains unchanged and is assumed to be uniform across all regions. This rate variable could fluctuate across regions on the basis of the available local control resources, and it is possible to capture such behavior in the model; however, this is outside the scope of this particular study.

Local-scale outbreak models are influenced by network flows. Specifically, for each compartment, the number of passengers in the flow between two regions is assumed to be directly proportional to its percentage in the population of the origin of travel. That is,

$$S_{ij,t+1} = f_{ij}\frac{S_{i,t}}{N_{i,t}} \qquad \forall i \in V, j \in \theta(i) \qquad \forall t \in T \tag{8}$$

$$I_{ij,t+1} = f_{ij}\frac{I_{i,t}}{N_{i,t}} \qquad \forall i \in V, j \in \theta(i) \qquad \forall t \in T \tag{9}$$

$$R_{ij,t+1} = f_{ij}\frac{R_{i,t}}{N_{i,t}} \qquad \forall i \in V, j \in \theta(i) \qquad \forall t \in T \tag{10}$$

where $S_{ij,t}$, $I_{ij,t}$, and $R_{ij,t}$ are the number of individuals in each compartment S, I, and R traveling from node i to node j at time t, respectively.

To ensure that the sum of traveling individuals in each compartment is equal to the total number of traveling individuals, the following is imposed:

$$f_{ij} = S_{ij,t} + I_{ij,t} + R_{ij,t} \qquad \forall i \in V \qquad \forall t \in T \tag{11}$$

These traveling individuals are next incorporated into the local outbreak model; thus Equations 5, 6, and 7 are modified to

$$S_{i,t+1} - S_{i,t} = -\frac{\beta_i I_{i,t} S_{i,t}}{N_{i,t}} + \sum_{j\in\theta(i)} S_{ji,t} - \sum_{j\in\theta(i)} S_{ij,t} \qquad \forall i \in V \qquad \forall t \in T \tag{12}$$

$$I_{i,t+1} - I_{i,t} = \frac{\beta_i I_{i,t} S_{i,t}}{N_{i,t}} - \gamma I_{i,t} + \sum_{j\in\theta(i)} I_{ji,t} - \sum_{j\in\theta(i)} I_{ij,t} \qquad \forall i \in V \qquad \forall t \in T \tag{13}$$

$$R_{i,t+1} - R_{i,t} = \gamma I_{i,t} + \sum_{j\in\theta(i)} R_{ji,t} - \sum_{j\in\theta(i)} R_{ij,t} \qquad \forall i \in V \qquad \forall t \in T \tag{14}$$

For each region, the compartments are initialized with input data representative of the local outbreak state at the beginning of the period of interest (i.e., $N_{i,0}$, $S_{i,0}$, $I_{i,0}$, and $R_{i,0}$ for each region i). It is also known that any change in the total population of a region is caused by the cumulative change in all compartments. These two relationships can be written as

$$N_{i,t+1} - N_{i,t} = S_{i,t+1} - S_{i,t} + I_{i,t+1} - I_{i,t} + R_{i,t+1} - R_{i,t} \qquad \forall i \in V \qquad \forall t \in T \tag{15}$$

$$N_{i,0} = S_{i,0} + I_{i,0} + R_{i,0} \qquad \forall i \in V \tag{16}$$

Note that if one substitutes Equations 12, 13, and 14 into the right-hand side of Equation 15, then uses Equation 11, the following relationship is found:

$$N_{i,t+1} - N_{i,t} = \sum_{j\in\theta(i)} f_{ji} - \sum_{j\in\theta(i)} f_{ij} \qquad \forall i \in V \qquad \forall t \in T \tag{17}$$

This relationship states that the change in the total local population of a node is equal to the difference of the total outgoing flow and the total incoming flow into the node, a hidden flow conservation condition at any node in the network.

So far, the structure of the multiscale model used to depict disease transmission in the air travel network has been established. This multiscale model can then be used to assess the epidemic outcome when control measures are applied to the network.

Outbreak Control Problem Definition

The coupled multiscale model is used as the lower-level model in the resource allocation problem (i.e., the outbreak control problem). For each control resource allocation strategy, the multiscale model can be run to generate corresponding outcomes. The objective of the upper-level model is to find the optimal outbreak control strategy to minimize the risk of infection spread for the network at the observation time t_{obs}. This optimization is subject to a budget constraint placed on the total amount of control resources available. The distribution of the resources has three fundamental dimensions: spatial (location), temporal (when control is active), and volume (how much to distribute at each location). Given the large solution space, this issue poses a challenging problem to solve for.

The control method explored in this model is incoming passenger screening at designated airports. It is assumed that if any arriving infected passengers are caught during the screening process, they are quarantined from the rest of population at their destination (i.e., they remain under care and surveillance until they are no longer infectious). Thus these infected passengers will not spread infection any further and can therefore be treated as removed from the population in which they are detected (i.e., they are immediately changed from an infected to recovered state). For infected passengers not successfully identified during the screening process, their recovery will still be governed by the recovery rate γ.

When control is implemented at a node i, the incoming passenger flows denoted by f_i^+ from Equation 4 are subject to passenger screening control. The control variable is expressed as a ratio with value between 0 and 1, indicating the percentage of infected passengers caught by the screening process at each location. The control variables are written as

$$x_{i,t} \in [0,1] \qquad \forall i \in V \qquad \forall t \in T \tag{18}$$

The time step subscript belongs to the set T, thus implying that control can be implemented at any time, including $t = 0$.

The imperfect control (ratio < 1) can be interpreted as a result of either limitations of available screening equipment technology (i.e., all passengers are screened but only a fraction of infected passengers are identified) or limitations in personnel (e.g., it may not be feasible to screen all passengers), so only a percentage of those infected can be detected even if the screening technology is perfect. In reality it is likely both factors would be in effect, limiting the percentage of infected passengers detected. This control variable can capture the combined effect of these two factors.

The control is indexed by node number and time step, therefore indicating where and when to implement control. How much to distribute is indicated by the actual value of $x_{i,t}$. Hence all three dimensions of variation of the control strategies have been captured with this variable. This control variable should be incorporated in the spread of the epidemic at the local scale, since the infected passengers move from the infected compartment to the recovered compartment at the destination region. Therefore, Equations 13 and 14 can be modified to be

$$I_{i,t+1} - I_{i,t} = \frac{\beta_i I_{i,t} S_{i,t}}{N_{i,t}} - \gamma I_{i,t} + (1 - x_{i,t}) \sum_{j\in\theta(i)} I_{ji,t} - \sum_{j\in\theta(i)} I_{ij,t} \qquad \forall i \in V \qquad \forall t \in T \tag{19}$$

$$R_{i,t+1} - R_{i,t} = \gamma I_{i,t} + \sum_{j\in\theta(i)} R_{ji,t} - \sum_{j\in\theta(i)} R_{ij,t} + x_{i,t} \sum_{j\in\theta(i)} I_{ji,t} \qquad \forall i \in V \qquad \forall t \in T \tag{20}$$

This step is intuitive because at every time step, $x_{i,t}\sum_{j\in\theta(i)} I_{ji,t}$ incoming infected passengers from the infected compartment are moved to the recovered compartment, exactly as described before. With the influence of control built into the multiscale lower-level outbreak model, the upper-level decision model can be used to evaluate various resource allocation policies. In this work, resources are distributed within the air travel network, and the impact of each in mitigating the spread of a current ongoing outbreak can be assessed.

Multiple possible objective functions can be defined to capture the risk of an epidemic. The objective studied in this paper is to minimize the total number of individuals affected by the epidemic in the entire network. If examined at the final time step t_{obs}, the number of individuals affected include those who are currently infected and those who were previously infected but have since recovered. Therefore, the objective is written as

$$Z_{IR} = \min \sum_{i\in V} \sum_{t\in T} (I_{i,t} + R_{i,t}) \tag{21}$$

The optimal outcome in this case is the resource allocation strategy that minimizes the number of individuals affected by the epidemic, while its cost does not exceed a fixed budget. In this work the cost incurred is assumed to be location specific (e.g., airport), a function of the number of incoming passengers, and the ratio of control applied. The total sum of the cost incurred in the entire network over the set of all nodes should not exceed the total budget. Let $\boldsymbol{x}_i = [x_{i,t}]_{t\in T\cup\{0\}}$ be the vector of control variables at node $i \in V$; then

$$\sum_{i\in V} h_i(\boldsymbol{x}_i, f_i^+) \le B \tag{22}$$

where h_i is the cost function at node i and B is the total budget available.

The objective is simply to quantify a relative cost and performance across a range of control strategies, which can then be ranked according to each metric, as well as cost-efficiency. For the purposes of this work, consider a simple two-part cost function that accounts for an upfront fixed cost of capital investment for the setup equipment, personnel, and procedures, and a daily service cost for implementing passenger screening. A general functional form that reflects these characteristics is the following:

$$h_i(\boldsymbol{x}_i, f_i^+) = \mathbf{1}_{(0,\infty)}\left(\sum_{t\in T} x_{i,t}\right) c_i + f_i^+ \sum_{t\in T} g_i(x_{i,t}) \tag{23}$$

The first term captures the fixed cost; $\mathbf{1}_{(0,\infty)}\,(\sum_{t\in T} x_{i,t})$ is an indicator function that takes on the value of 1 if any amount of control is implemented at node i at any point in time, and 0 otherwise. The term c_i is assumed to be the amount of capital investment for each node, if control is implemented. The second term captures the service cost; f_i^+ is the number of incoming passengers to node i at time t, and this is multiplied by a function $g_i(x_{i,t})$, which defines the cost to screen per passenger, if the control variable $x_{i,t}$ is set to be at a certain level. It is assumed that this function is nonlinear in nature because of a rising marginal cost as a higher degree of control is placed on a node (e.g., it would be hard to ensure that most of the infected are detected, and ensuring 100% infected are detected would be prohibitively costly, if possible) (*32*). It is also assumed that control can be implemented at any point in time until the end of the modeling process when $t = t_{\text{obs}}$, and vary over time.

With the optimization framework introduced, the formulations of the upper-level decision problem and the lower-level multiscale outbreak model are presented together in the next section. Thus the main contribution of this work is this bilevel modeling framework to facilitate optimized decision making, while accounting for multiscale infection dynamics.

MATHEMATICAL FORMULATION

Upper-Level Formulation

$$Z_{IR} = \min \sum_{i\in V}\sum_{t\in T} I_{i,t} + R_{i,t} \tag{24}$$

subject to

$$\sum_{i\in V} h_i\left(\boldsymbol{x}_i, f_i^+\right) \le B \tag{25}$$

Lower-Level Formulation

$$S_{ij,t+1} = f_{ij}\,\frac{S_{i,t}}{N_{i,t}} \qquad \forall i\in V,\ j\in\theta(i) \qquad \forall t\in T \tag{26}$$

$$I_{ij,t+1} = f_{ij}\,\frac{I_{i,t}}{N_{i,t}} \qquad \forall i\in V,\ j\in\theta(i) \qquad \forall t\in T \tag{27}$$

$$R_{ij,t+1} = f_{ij}\,\frac{R_{i,t}}{N_{i,t}} \qquad \forall i\in V,\ j\in\theta(i) \qquad \forall t\in T \tag{28}$$

$$f_{ij} = S_{ij,t} + I_{ij,t} + R_{ij,t} \qquad \forall i\in V,\ j\in\theta(i) \qquad \forall t\in T \tag{29}$$

$$S_{i,t+1} - S_{i,t} = -\frac{\beta_i I_{i,t} S_{i,t}}{N_{i,t}} + \sum_{j\in\theta(i)} S_{ji,t} - \sum_{j\in\theta(i)} S_{ij,t} \qquad \forall i\in V \qquad \forall t\in T \tag{30}$$

$$I_{i,t+1} - I_{i,t} = \frac{\beta_i I_{i,t} S_{i,t}}{N_{i,t}} - \gamma I_{i,t} + \left(1 - x_{i,t}\right)\sum_{j\in\theta(i)} I_{ji,t} - \sum_{j\in\theta(i)} I_{ij,t} \qquad \forall i\in V \qquad \forall t\in T \tag{31}$$

$$R_{i,t+1} - R_{i,t} = \gamma I_{i,t} + \sum_{j\in\theta(i)} R_{ji,t} - \sum_{j\in\theta(i)} R_{ij,t} + x_{i,t}\sum_{j\in\theta(i)} I_{ji,t} \qquad \forall i\in V \qquad \forall t\in T \tag{32}$$

$$N_{i,t+1} - N_{i,t} = S_{i,t+1} - S_{i,t} + I_{i,t+1} - I_{i,t} + R_{i,t+1} - R_{i,t} \qquad \forall i\in V \qquad \forall t\in T \tag{33}$$

$$N_{i,0} = S_{i,0} + I_{i,0} + R_{i,0} \qquad \forall i\in V \tag{34}$$

$$x_{i,t} \in [0,1] \qquad \forall i\in V \qquad \forall t\in T \tag{35}$$

Observe that the flows between regions f_{ij} are assumed to be time-independent (i.e., interregional flows are constant). This means the same amount of flow between each node pair is expected throughout the duration of the model simulation process. This assumption could be relaxed when detailed data are available to reflect variation in flows.

CASE STUDY

A case study using the worldwide air travel network is presented in this section. A hypothetical epidemic outbreak is assumed to emerge from within the United States, and different control resource allocation strategies are explored and evaluated. The spread of infection is modeled at the global scale; however, the control decisions are only considered for U.S. airports. Thus the strategies are evaluated at the U.S. level (i.e., only U.S. infections are accounted for in the objective function).

Data

The 2015 global air travel data provided by the International Air Transport Association (*33*) are used to build the global air traffic network used for the lower-level multiscale outbreak model. The aggregate travel volumes for the month of June, July, and August are used. In this network there are more than 500,000 distinct travel routes, with 3,766 distinct nodes (airport of a local region). The travel volumes can be grouped to calculate the total outgoing and incoming volumes through each airport. A closer examination of the data shows that the 1,000 airports (out of a total of 3,766) account for approximately 95% of the total travel volume, which follows the scale-free nature of the air traffic network (*3*). That is, a few hubs are very well connected, while the rest are sparsely connected. In this paper, the analysis is focused on the truncated network with these 1,000 airports, which results in 141 airports accounted for in the United States. Although this is a simplification on the network structure, the effects are minimal because the major airports and a majority of the travel volume are captured. To fit the purpose of building a model that could capture the dynamics of an emerging outbreak at its early stages, the flows are disaggregated to the average daily flows between airports. The population data at each airport are obtained from LandScan (*34*). A 50-km radius was used to estimate the local population for each city.

Experiment Design

Control strategy allocation has three important fundamental aspects: where to allocate control, how much control to allocate to each location, and when to allocate control. The "when to allocate" aspect is not explored in this paper. Intuitively, the optimal time to implement control is closely related to the dynamic progression of the epidemic and is a topic of much complexity in itself. For the purpose of this study, and because of space limitations, all control measures are assumed to be implemented at time step $t = 0$ and kept at their fixed levels until t_{obs}. The other two aspects, "where to allocate" and "how much to allocate," are explored in the following sections.

For the purposes of this study, a hypothetical epidemic outbreak sourced in Austin, Texas, is considered. A set of control strategies, which vary in number, location, and level of control, is defined and evaluated. In each strategy it is assumed that $t_{obs} = 50$, that is, $T \in \{0, 1, 2, \ldots, 50\}$. This time indicates how far in the future the state of the outbreak is evaluated. The relatively short timeline is representative of the early stages of an emerging outbreak, which is the intended application of the model. However, the observation time can be varied to suit the need of the modeler. The outbreak modeled is assumed to be caused by a highly contagious disease, similar to the recent Ebola outbreak. The recovery rate is assumed to be $\gamma = 0.178$, which is equal to an infectious period of approximately 5.6 days. It is assumed that 100 individuals are already infected in Austin (i.e., at time $t = 0$).

As noted previously, the local transmission rate β_i for each region increases linearly with population density and is assumed to be bounded. For this network it is assumed that the lowest transmission rate for a region is 0.2 (corresponding to the region at the 5th percentile in population size), and the highest value of the rate is 0.35 (corresponding to the region at the 95th percentile), and for regions in between the transmission rate is interpolated linearly between these two extreme points, based on population density. These parameter values are consistent with the recent Ebola outbreak (*35*).

Evaluation of Control Strategy Location Selection

Intuitively, applying perfect control at the locations directly connected to the source is the most effective strategy. However, it could be prohibitively expensive to apply control at all airports connected to a given outbreak source location because of the high connectivity of the air traffic network and even more so if there were multiple sources. To illustrate and assess the impact of different outbreak control strategies, the authors propose a range of strategies for selecting a subset of airports at which to implement control and compare them with respect to their effectiveness in reducing the outbreak impact. The five strategies are named random, largest populations, most connected, most through travel, and largest outbreak. For each strategy, 20 locations are selected. The methods by which these 20 locations are selected for each strategy are outlined in Table 1. A baseline strategy is also included for comparison with other strategies. The control strategies are assumed to be implemented on candidate locations in the United States, with Austin the noted source city.

TABLE 1 Selection Methods for Location-Based Control Strategies

Location-Based Control Strategy	Selection Method
Baseline	No control is placed. This is the baseline scenario for the basis of comparisons with others.
Random	Randomly select a set of 20 airports connected to source node.
Largest populations	Rank all airports connected to source node on the basis of their local population and select the top 20 airports.
Most connected	Rank all airports connected to source node on the basis of their volume of passenger flows from source node and select the top 20 airports.
Most through travel	Rank all airports connected to source node on the basis of their total passenger throughput (total of incoming and outgoing travelers) and select the top 20 airports.
Largest outbreak	Run the multiscale simulation model for the baseline case (without control treatment) and rank all airports connected to the source node on the basis of the outbreak size (number of individuals infected and recovered), at $t_{obs} = 50$ in each city, and select the top 20 airports.

Each location-based control strategy is evaluated across a range of control variables $x_{i,t}$ from 0 to 1, at 0.1 increments. Recall that the value of the control variable is the percentage of incoming passengers screened and detected at a particular location. Hence $x_{i,t} = 0$ (0%) represents that no control resource will be placed on a region, and $x_{i,t} = 1$ (100%) represents that all infected passengers coming into this region will be detected and quarantined. The same level of control is assumed to be placed across all control locations, allowing a comparison of the impact of different levels of control across location-based strategies. The results are illustrated in Figure 1.

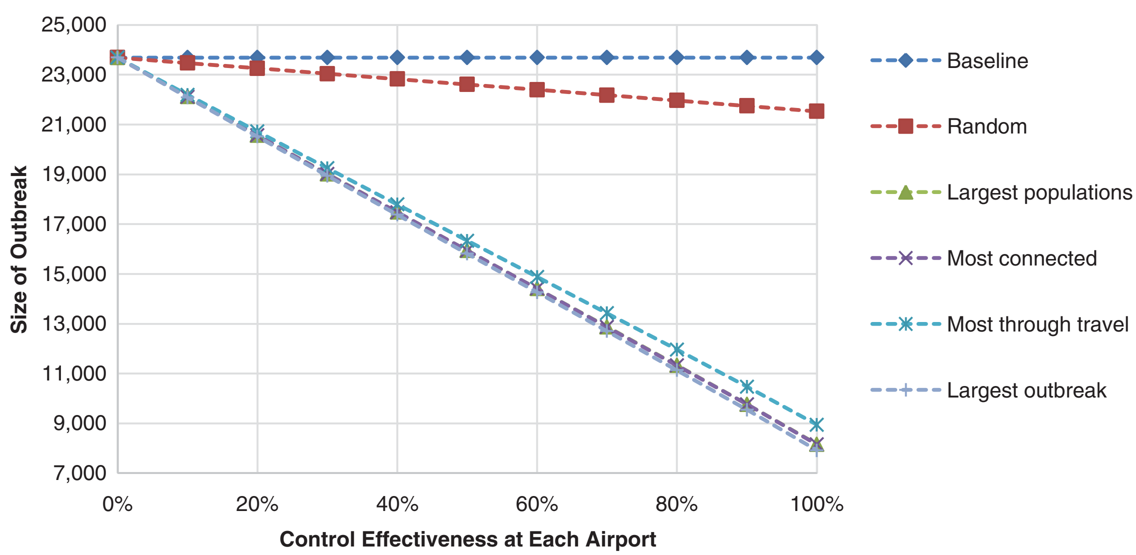

FIGURE 1 Total number of people ever infected for each strategy (size of outbreak at $t = 50$).

The x-axis represents the control level and the y-axis represents the outbreak size within the United States. Each data series represents a location strategy, and each point on the data series corresponds to a particular location control level strategy. It should be noted that the dashed lines connecting the points are drawn to distinguish between data series and do not signify interpolation.

The baseline data series in Figure 1 serves as a basis of comparison with other strategies, representing the number of people affected by the epidemic when no control treatment is implemented. From these results, the reduction in the number of affected individuals for each strategy can be assessed.

All strategies reveal a linear relationship with the control variable, with a higher level of control expectedly corresponding to a greater reduction in outbreak size. The random strategy causes the least amount of reductions in outbreak size, while the most through travel strategy results in much larger reductions. The most connected, largest population, and largest outbreak strategies show even better outcomes. The performance of these three strategies is similar because the locations selected using these three are similar, meaning many places rank high in multiple metrics. The cost-efficiencies of these three strategies are much higher than that of the random strategy (i.e., the same amount of reduction in the number of people affected would require much fewer resources). Out of these three strategies, the largest outbreak strategy has the highest cost-efficiency.

Overall, the results illustrate the importance of the selection of control locations, especially compared with randomly selected locations. However, there is not much difference in the results of the best-performing strategies, because of many locations meeting multiple criteria for the best location selection. This finding suggests that the location-based selection of the best-performing strategies is rather robust and can be selected by using a set of heuristic criteria. Similar results were obtained when the number of control locations selected was changed to 10 and 30, but the results are not included in this paper because of size limitations. The analysis presented in the next section seeks to explore how varying the level of control across the best locations affects both cost and efficiency of the control.

Evaluation of Control Levels and Control Costs

This section explores the third aspect of control resource allocation: how much control resource should be allocated to each location? Given that the best-performing locations to implement control can be selected, one can then examine the cost-efficiencies of the control strategies by keeping the set of chosen locations constant and varying the levels of control implemented. The cost-efficiency metric used is explained in the discussion of the results later in this section. From this the relationship between the cost-efficiencies and the levels of controls can be observed. The 20 nodes from the largest outbreak set were chosen because of their good performance in outbreak size reduction, as shown in the previous section. The control resources are assumed to be implemented on these 20 candidate locations (Table 2).

The cost of each control strategy is computed on the basis of Equation 23, and for this study $c_i = 10f_i^+$ and $g(x_{i,t}) = x_{i,t} + x_{i,t}$ were chosen as the functions for capital investment and screening cost. The factor of 10 was chosen so that the capital investment would be a nontrivial part of the total cost. The function $g(x_{i,t}) = x_{i,t}^4/2 + x_{i,t}$ was chosen because as $x_{i,t}$ increases from 0 to 1, the value of the function increases slowly initially, but quite rapidly as $x_{i,t} \rightarrow 1$. When $x_{i,t}$ takes on its maximum value of 1, the value of the function is 1.5, meaning the cost of implementing full control would be 50% more in total compared with the case where it is assumed that the costs are scaled linearly with control ratio [e.g., $g(x_{i,t}) = x_{i,t}$]. Note that to obtain the real cost of the control measure, this function should be further multiplied by a factor that could convert this scaled control ratio into cost per passenger at that ratio. This factor is assumed to be 1 for the purposes of this analysis. These chosen functional forms are used to explore how possible scenarios may play out given a reasonably assumed cost function and do not represent any specific monetary units. Estimating the exact cost of equipment and personnel for airport screening is beyond the scope of this study.

TABLE 2 Top 20 Candidate Locations for Control Measures

Airport (IATA code)	City (Airport)	Population (within 50-km buffer of airport)	Passenger Flow (90 days)
LGA	New York (La Guardia)	15,763,005	293,246
LAX	Los Angeles	10,244,614	179,951
ORD	Chicago (O'Hare)	7,807,107	148,741
OAK	Oakland	5,459,164	145,810
DFW	Dallas (Fort Worth)	6,040,552	98,812
DCA	Washington (National)	5,634,567	94,598
LGB	Long Beach	11,239,720	45,097
PHL	Philadelphia	5,565,904	52,196
BWI	Baltimore	5,296,240	48,395
ATL	Atlanta	4,020,075	85,918
SAN	San Diego	4,568,841	54,717
FLL	Fort Lauderdale	4,281,812	130,539
BOS	Boston	4,398,340	91,347
PHX	Phoenix	4,050,658	70,678
IAH	Houston (Intercontinental)	5,298,753	77,715
DEN	Denver	2,695,321	91,094
SEA	Seattle	3,468,857	83,493
SJC	San Jose	3,741,393	27,436
DTW	Detroit	4,011,874	47,130
LAS	Las Vegas	2,014,875	99,829

NOTE: IATA = International Air Transport Association.

To demonstrate the cost-efficiencies of the levels of control applied, it is again assumed, as in the previous section, that the same level of control ratio is applied at each of the 20 selected nodes. This study explored the cost-efficiencies of applying incremental levels of controls on these nodes. These cost-efficiencies are shown in Scenario 1 to Scenario 10 in Table 3.

The "Total Reduction in Outbreak Size" column of the results represents the reduction in outbreak size at $t_{obs} = 50$ compared with the baseline scenario. The "Number of Quarantined Passengers" is the total number of infected passengers detected at the nodes being selected for passenger screening. The "Normalized Cost of Strategy" column shows the normalized cost (as a proportion of the strategy with the maximum cost) incurred by each strategy, as calculated from the cost function defined in Equation 23. "Normalized Cost Efficiency" is the metric used to measure the cost-efficiency of each strategy. It is calculated by dividing the cost of each strategy by the "Total Reduction in Outbreak Size" for the corresponding strategy, thus providing the average cost per prevented infection, again normalized to the maximum value across strategies.

TABLE 3 Results with Varying Levels of Control

Scenario	Control Strategy	Total Reduction in Outbreak Size (within United States)	Number of Quarantined Passengers	Normalized Cost of Strategy	Normalized Cost Efficiency
0	No control applied	0	0	0	na
1	$x_{i,t} = 0.1$ at all 20 nodes	1,597	30	0.18	0.91
2	$x_{i,t} = 0.2$ at all 20 nodes	3,174	57	0.24	0.61
3	$x_{i,t} = 0.3$ at all 20 nodes	4,747	80	0.30	0.51
4	$x_{i,t} = 0.4$ at all 20 nodes	6,307	99	0.36	0.47
5	$x_{i,t} = 0.5$ at all 20 nodes	7,873	113	0.43	0.45
6	$x_{i,t} = 0.6$ at all 20 nodes	9,424	125	0.51	0.44
7	$x_{i,t} = 0.7$ at all 20 nodes	10,987	134	0.60	0.45
8	$x_{i,t} = 0.8$ at all 20 nodes	12,551	141	0.71	0.46
9	$x_{i,t} = 0.9$ at all 20 nodes	14,141	146	0.84	0.49
10	$x_{i,t} = 1.0$ at all 20 nodes	15,775	154	1.00	0.52
11	$x_{i,t} = 0.9$ for first 10 nodes, and $x_{i,t} = 0.1$ for the rest	12,283	109	0.58	0.39
12	$x_{i,t} = 0.1$ for first 10 nodes, and $x_{i,t} = 0.9$ for the rest	3,586	120	0.44	1.00
13	$x_{i,t} = 0.9$ for first 10 nodes, and $x_{i,t} = 0.0$ for the rest	12,056	104	0.51	0.35

NOTE: na = not applicable.

Scenario 0 shows the baseline when no control is applied. Scenario 1 to Scenario 10 show incremental increases in the levels of control applied on the 20 largest outbreak locations. The cost and the number of passengers quarantined increase with the levels of control applied. The normalized cost-efficiency is initially high when $x_{i,t} = 0.1$ for all nodes, but it decreases as the levels of control increase, and eventually rises again. The initial high cost is caused by the significant amount of capital investment required, making it inefficient to apply a low level of control on all locations. If higher levels of control are implemented, then they are comparatively more cost-efficient. However, as the levels of control approach very high thresholds, it becomes increasingly costly to ensure that such a large percentage of infected passengers can be detected, hence the rise in normalized cost-efficiency as $x_{i,t}$ approaches 1. The cost-efficiency comparison of Scenario 1 to Scenario 10 shows two important observations about control resource allocation. The first is that because of the initial investment required to set up control at nodes, implementing higher control levels on nodes being controlled could improve the cost-efficiency of a strategy. The second is that increasing the levels of control beyond a certain point could decrease the cost-efficiency by so much that it may offset the benefit of the previously mentioned improvement. This point illustrates that there is a balancing point for when cost-efficiency would be the highest, depending on the cost function and the input of the model. It is not trivial to determine where this optimal point is.

Next this paper explores whether better cost-efficiency can be achieved by allowing varying levels of control across all the selected regions, specifically, if focusing resources on a particular subset of regions can yield good strategies. Two scenarios are contrasted, as shown in Scenario 11 and Scenario 12. In Scenario 11, control resources are allocated to prioritize the control in the first 10 nodes by ranking (largest outbreak). In Scenario 12, control resources are invested in the second half of the 20 nodes. The former is shown to be much more cost-efficient than the latter and also more cost-efficient than Scenarios 1 to 10. Thus prioritizing the allocation of control resources to certain locations may yield better results than simple strategies that keep control levels uniform across candidate locations.

Scenario 13 offers an interesting comparison with Scenario 11. In Scenario 13, the first 10 nodes are assigned the same control levels as those in Scenario 11, but the second half of the 20 nodes are not controlled at all. This frees up the capital cost spent on these nodes, resulting in a higher cost-efficiency. This example shows that epidemic control outcome can possibly be improved by eliminating inefficient capital investment allocations.

It is worth noting that having high cost-efficiency may not imply that a strategy is necessarily better, depending on the total amount of budget available. For example, if one compares Scenario 11 and Scenario 12, even though the strategy in Scenario 11 is much more cost-efficient, the total cost of this strategy is much higher than that in Scenario 12. Therefore, depending on the budget, this strategy may not even be in the possible pool of candidate strategies. In an optimization framework, the best strategy should be the one that is the most cost-efficient within the defined cost budget.

CONCLUSIONS

This paper proposes a multiscale network modeling framework that simultaneously captures the role of local and interregional infection dynamics in the global spread of an epidemic within a decision-making framework that seeks to identify the optimal outbreak control strategy. A case study is conducted on the U.S. air travel network. Outputs from the model provide a means to quantify, evaluate, and rank control strategies with respect to efficiency and cost-efficiency. Future work will focus on developing efficient optimization algorithms to select the most efficient and affordable outbreak control strategies while accounting for all degrees of freedom. Different functional forms for the cost function and objective functions will be considered.

ACKNOWLEDGMENT

The authors thank the National Health and Medical Research Council, Australia, for funding.

REFERENCES

1. U.S. to Screen Passengers from West Africa for Ebola at 5 Airports. *TIME.* http://time.com/3482094/ebola-us-west-africa-airports/. Accessed June 21, 2016.
2. Kermack, W.O., and A.G. McKendrick. A Contribution to the Mathematical Theory of Epidemics. *Proceedings of the Royal Society of London A: Mathematical, Physical and Engineering Sciences,* Vol. 115, No. 772, 1927, pp. 700–721. https://doi.org/10.1098/rspa.1927.0118.
3. Guimerà, R., S. Mossa, A. Turtschi, and L.N. Amaral. The Worldwide Air Transportation Network: Anomalous Centrality, Community Structure, and Cities' Global Roles. *Proceedings of the National Academy of Sciences of the United States of America,* Vol. 102, No. 22, 2005, pp. 7794–7799. https://doi.org/10.1073/pnas.0407994102.
4. Hufnagel, L., D. Brockmann, and T. Geisel. Forecast and Control of Epidemics in a Globalized World. *Proceedings of the National Academy of Sciences of the United States of America,* Vol. 101, No. 42, 2004, pp. 15124–15129. https://doi.org/10.1073/pnas.0308344101.
5. Grais, R.F., J.H. Ellis, A. Kress, and G.E. Glass. Modeling the Spread of Annual Influenza Epidemics in the U.S.: The Potential Role of Air Travel. *Health Care Management Science,* Vol. 7, No. 2, 2004, pp. 127–134. https://doi.org/10.1023/B:HCMS.0000020652.38181.da.
6. Broeck, W.V., C. Gioannini, B. Gonçalves, M. Quaggiotto, V. Colizza, and A. Vespignani. The GLEaMviz Computational Tool, a Publicly Available Software to Explore Realistic Epidemic Spreading Scenarios at the Global Scale. *BMC Infectious Diseases,* Vol. 11, No. 1, 2011, p. 37.
7. Ajelli, M., B. Gonçalves, D. Balcan, V. Colizza, H. Hu, J.J. Ramasco, S. Merler, and A. Vespignani. Comparing Large-Scale Computational Approaches to Epidemic Modeling: Agent-Based Versus Structured Metapopulation Models. *BMC Infectious Diseases,* Vol. 10, No. 1, 2010, p. 190.
8. Tizzoni, M., P. Bajardi, C. Poletto, J.J. Ramasco, D. Balcan, B. Gonçalves, N. Perra, V. Colizza, and A. Vespignani. Real-Time Numerical Forecast of Global Epidemic Spreading: Case Study of 2009 A/H1N1pdm. *BMC Medicine,* Vol. 10, No. 1, 2012, p. 165. https://doi.org/10.1186/1741-7015-10-165.
9. Balcan, D., V. Colizza, B. Gonçalves, H. Hu, J.J. Ramasco, and A. Vespignani. Multiscale Mobility Networks and the Spatial Spreading of Infectious Diseases. *Proceedings of the National Academy of Sciences of the United States of America,* Vol. 106, No. 51, 2009, pp. 21484–21489. https://doi.org/10.1073/pnas.0906910106.
10. Balcan, D., B. Gonçalves, H. Hu, J.J. Ramasco, V. Colizza, and A. Vespignani. Modeling the Spatial Spread of Infectious Diseases: The Global Epidemic and Mobility Computational Model. *Journal of Computational Science,* Vol. 1, No. 3, 2010, pp. 132–145. https://doi.org/10.1016/j.jocs.2010.07.002.
11. Gardner, L., D. Fajardo, and S. Waller. Inferring Infection-Spreading Links in an Air Traffic Network. *Transportation Research Record: Journal of the Transportation Research Board,* No. 2300, 2012, pp. 13–21. https://dx.doi.org/10.3141/2300-02.
12. Brockmann, D., and D. Helbing. The Hidden Geometry of Complex, Network-Driven Contagion Phenomena. *Science,* Vol. 342, No. 6164, 2013, pp. 1337–1342. https://doi.org/10.1126/science.1245200.
13. Gardner, L., and S. Sarkar. A Global Airport-Based Risk Model for the Spread of Dengue Infection via the Air Transport Network. *PLoS One,* Vol. 8, No. 8, 2013, p. e72129. https://doi.org/10.1371/journal.pone.0072129.
14. Gardner, L.M., D. Fajardo, S.T. Waller, O. Wang, and S. Sarkar. A Predictive Spatial Model to Quantify the Risk of Air-Travel-Associated Dengue Importation into the United States and Europe. *Journal of Tropical Medicine,* Vol. 2012, 2012, p. e103679. https://doi.org/10.1155/2012/103679.
15. Richter, A., M.L. Brandeau, and D.K. Owens. An Analysis of Optimal Resource Allocation for Prevention of Infection with Human Immunodeficiency Virus (HIV) in Injection Drug Users and Non-users. *Medical Decision Making,* Vol. 19, No. 2, 1999, pp. 167–179. https://doi.org/10.1177/0272989X9901900207.
16. Brandeau, M.L., G.S. Zaric, and A. Richter. Resource Allocation for Control of Infectious Diseases in Multiple Independent Populations: Beyond Cost-Effectiveness Analysis. *Journal of Health Economics,* Vol. 22, No. 4, 2003, pp. 575–598. https://doi.org/10.1016/S0167-6296(03)00043-2.
17. Zaric, G.S., and M.L. Brandeau. Resource Allocation for Epidemic Control Over Short Time Horizons. *Mathematical Biosciences,* Vol. 171, No. 1, 2001, pp. 33–58. https://doi.org/10.1016/S0025-5564(01)00050-5.
18. Greenhalgh, D. Control of an Epidemic Spreading in a Heterogeneously Mixing Population. *Mathematical Biosciences,* Vol. 80, No. 1, 1986, pp. 23–.45. https://doi.org/10.1016/0025-5564(86)90065-9.
19. Greenhalgh, D. Some Results on Optimal Control Applied to Epidemics. *Mathematical Biosciences,* Vol. 88, No. 2, 1988, pp. 125–158. https://doi.org/10.1016/0025-5564(88)90040-5.
20. Blount, S., A. Galambosi, and S. Yakowitz. Nonlinear and Dynamic Programming for Epidemic Intervention. *Applied Mathematics and Computation,* Vol. 86, No. 2–3, 1997, pp. 123–136. https://doi.org/10.1016/S0096-3003(96)00177-4.
21. Müller, J. Optimal Vaccination Patterns in Age-Structured Populations. *SIAM Journal on Applied Mathematics,* Vol. 59, No. 1, 1998, pp. 222–241. https://doi.org/10.1137/S0036139995293270.
22. Zaric, G.S., and M.L. Brandeau. Dynamic Resource Allocation for Epidemic Control in Multiple Populations. *Mathematical Medicine and Biology,* Vol. 19, No. 4, 2002, pp. 235–255. https://doi.org/10.1093/imammb/19.4.235.
23. Ndeffo Mbah, M.L., and C.A. Gilligan. Resource Allocation for Epidemic Control in Metapopulations. *PLoS One,* Vol. 6, No. 9, 2011, p. e24577. https://doi.org/10.1371/journal.pone.0024577.
24. Deng, Y., S. Shen, and Y. Vorobeychik. Optimization Methods for Decision Making in Disease Prevention and Epidemic Control. *Mathematical Biosciences,* Vol. 246, No. 1, 2013, pp. 213–227. https://doi.org/10.1016/j.mbs.2013.09.007.
25. Cohen, R., S. Havlin, and D. ben-Avraham. Efficient Immunization Strategies for Computer Networks and Populations. *Physical Review Letters,* Vol. 91, No. 24, 2003, p. 247901. https://doi.org/10.1103/PhysRevLett.91.247901.
26. Borgs, C., J. Chayes, A. Ganesh, and A. Saberi. How to Distribute Antidote to Control Epidemics. *Random Structures and Algorithms,* Vol. 37, No. 2, 2010, pp. 204–222.
27. Chung, F., P. Horn, and A. Tsiatas. Distributing Antidote Using Page Rank Vectors. *Internet Mathematics,* Vol. 6, No. 2, 2009, pp. 237–254. https://doi.org/10.1080/15427951.2009.10129184.
28. Roy, S., A. Saberi, and Y. Wan. Designing Spatially Heterogeneous Strategies for Control of Virus Spread. *IET Systems Biology,* Vol. 2, No. 4, 2008, pp. 184–201. https://doi.org/10.1049/iet-syb:20070040.
29. Gourdin, E., J. Omic, and P. Van Mieghem. Optimization of Network Protection Against Virus Spread. In *Proceedings of the 8th International Workshop on the Design of Reliable Communication Networks,* Institute of Electrical and Electronic Engineers, Inc., Piscataway, N.J., 2011, pp. 86–93. https://doi.org/10.1109/DRCN.2011.6076889.
30. Preciado, V.M., M. Zargham, C. Enyioha, A. Jadbabaie, and G. Pappas. Optimal Vaccine Allocation to Control Epidemic Outbreaks in Arbitrary Networks. In *Proceedings of the 52nd IEEE Conference on Decision and Control,* Institute of Electrical and Electronic Engineers, Inc., Piscataway, N.J., 2013, pp. 7486–7491. https://doi.org/10.1109/CDC.2013.6761078.
31. Chen, N., L. Gardner, and D. Rey. Bilevel Optimization Model for the Development of Real-Time Strategies to Minimize Epidemic Spreading Risk in Air Traffic Networks. *Transportation Research Record: Journal of the Transportation Research Board,* No. 2569, 2016, pp. 62–69. https://dx.doi.org/10.3141/2569-07.
32. Selvey, L.A., C. Antão, and R. Hall. Evaluation of Border Entry Screening for Infectious Diseases in Humans. *Emerging Infectious Diseases,* Vol. 21, No. 2, 2015, pp. 197–201. https://doi.org/10.3201/eid2102.131610.
33. International Air Transport Association. http://www.iata.org/Pages/default.aspx. Accessed July 25, 2016.
34. LandScan Home. http://web.ornl.gov/sci/landscan/. Accessed July 25, 2016.
35. Althaus, C.L. Estimating the Reproduction Number of Ebola Virus (EBOV) During the 2014 Outbreak in West Africa. *PLoS Currents,* 2014. https://doi.org/10.1371/currents.outbreaks.91afb5e0f279e7f29e7056095255b288.

The contents of the paper are solely the responsibility of the administering institution, a participating institution, or individual authors and do not reflect the views of the National Health and Medical Research Council.

The Standing Committee on Aviation Security and Emergency Management peer-reviewed this paper.